

# Structural performance of severely damaged reinforced concrete beams after SRP repair

Hayder H. Alghazali<sup>1</sup>, Zuhair K. Al-Jaberi<sup>1</sup>, Zena R. Aljazeera<sup>2</sup>, John J. Myers<sup>3\*</sup>

<sup>1</sup>Graduate Research Student, Civil, Arch. and Envir. Engr, Missouri University of Science and Technology, Rolla, MO 65409, USA

<sup>2</sup>Lecturer, Nahrain University, Bagdad, Iraq

<sup>3</sup>Professor of Civil, Arch. and Envir. Engr and Associate Dean, Missouri University of Science and Technology, Rolla, MO 65409, USA (\*Corresponding and Presenting Author)

\*Corresponding author

DOI: 10.5185/amlett.2018.2153

www.vbripress.com/aml

## Abstract

To experimentally examine the ability of the steel reinforced polymer (SRP) in restoring the moment capacity compromised by damage in the main steel reinforcement, six full-scale reinforced concrete (RC) beams were designed to simulate impact damage from over height vehicle collision. The simulation was represented by concrete beams reinforced with discontinuous reinforcement (splice in maximum moment region) and tested until failure due to splice. The damaged concrete was repaired, and the SRP system (longitudinal soffit laminates and transverse U-wraps) was applied to restore the original moment capacity. All beams were 10 ft (3.0 m) in length, 18 in. (457 mm) in depth, and 12 in. (305 mm) in width. Different repairing configurations were investigated. The studied variables were the provided laminate area and the amount and distribution of U-wraps. The ultimate load capacity, deflection, and mode of failure were recorded during testing. The test results were compared to beam results with continuous reinforcement. It was concluded that the repairing beams with the SRP system can restore the damaged beams to a capacity similar to that of a non-damaged reinforced concrete (RC) beam with continuous reinforcement. Copyright © 2018 VBRI Press.

**Keywords:** Severely damaged beam, SRP system, splice, flexural capacity, over-height vehicle impact.

## Introduction

Advanced concrete and composite materials technology has advanced for use in infrastructure applications. Many infrastructure elements have been exposed to severe damages due to human and/or natural sources. Fire, explosive, over height vehicles collision, overweight loads are examples caused from human sources, while natural sources are represented by corrosion, earthquake, tornado, flooding, etc. The developed technologies have been facilitated in a way to repair such damaged structures and restore their ability to resist loads. Many researchers have studied the influence of using fiber reinforced polymers (FRP) in repairing existing infrastructure. Soudki et al. (2000) presented a study on the flexural performance of corroded RC beams that repaired using a patch mortar and FRP composites. The RC beams were subjected to 5%, 10%, and 15% mass losses of their longitudinal steel reinforcement. The beams were repaired with carbon-FRP at the tension zone with U-wrapped glass-FRP. The repaired beams showed an increase in the yield and ultimate strength of about 25% to 50% with a reduction in crack opening up to 88% [1]. Russo et al. (2000) studied the influence of using fiber reinforced plates for flexural repairing and carbon-FRP for shear enhancement of damaged

prestressed (PS) girder due to overheight vehicles. The test results showed a 12% increase in the moment capacity of the PS girder [2]. Klaiber et al. (2003) conducted a field demonstration project on repairing damaged PS girders due to overheight vehicles. The field experimental testing revealed that the damaged girder restored its load carrying capacity [3]. Haddad et al. (2008) used a steel and polypropylene fibers with high strength concrete to repair concrete damaged at the compression face and glass fiber reinforced sheets or ferrocement meshes to repair the tension face of the damaged beams. The enhancement in the ultimate load capacities for the repaired beams ranged between 99% and 126% of the control beam. In addition, the observed cracks were very fine through the flexural region [4]. El-Maaddawy et al. (2012) used a carbon-FRP with different end anchorages for retrofitting T-girders that were subjected to severe shear damages from overweight vehicles. It was found that the retrofitting FRP with end anchorages were able to restore the shear strength capacity of the original girders and demonstrated that additional shear resistance can be achieved based on the type of end anchorages employed [5]. The ductility and energy absorption were remarkably improved by one type of end anchors (thro-bolt anchors). Zhou et al. (2013) tested a repaired concrete-encased steel beams

with carbon-FRP or carbon-flex composite that subjected to fracture fatigue damages. Two repaired beams with carbon-flex composite showed a 68% restoration of their peak strength, a stabilization of crack growth, and a significant enhancement in their displacement ductility. However, the carbon-FRP composite was only able to restore the beams' capacity with a sharp failure ending without a sufficient displacement ductility [6]. Tigeli et al. (2013) investigated the effectiveness of combined using a patch mortar and carbon-FRP in repairing corroded RC beams. The test results revealed that an increase in the ultimate load capacities up to 50% for the repaired beams with patch mortar and carbon-FRP. While the patch mortar on its own failed to improve the beams' ultimate load capacities [7]. Pino et al. (2016) repaired PS girders subjected to impact damage of overweight vehicles. The repair method included the use of strand splicing and external high tensile strength fiber reinforcements (carbon-FRP or carbon-FRP and fiber reinforced cementitious composite, FRCM). The PS girder that was repaired with carbon-FRP exhibited an increase of 12% in its moment capacity with respect to the reference beam. On the other hand, the repaired PS girder with FRCM was prematurely damaged due to deck defects (saw cut) as a result the evaluation of the FRCM composite was unknown [8].

In this research an experimental study testing of six beams were conducted to evaluate the influence of the SRP system in restoring the load carrying capacity of RC beams after the impact of over height vehicle collision. This is the first study of its type using the SRP repair technology in reported literature to examine the feasibility of restoring capacity in a damaged lap splice (i.e. simulated impact damaged) region. The test parameters were included the effect of increasing the SRP laminate area, the U-wraps impact, and the influence of the U-wraps distribution.

## Experimental work

This work represents a part of an on-going research study whose main objective was to restore moment capacity to damaged tested RC beams. In this case study, a lap splice of the main reinforcement was provided in the higher moment region of a simply support beam (i.e. mid span location). It simulated the effect of damaged steel reinforcement within the critical moment region for a simply support RC beam when the reinforcement can be exposed to a severe impact or cutting.

Six beams were tested at Missouri University Science and Technology (Missouri S&T). All beams were 12 in. (305 mm) wide (b) with a total depth (h) of 18 in. (457 mm). In each of these beams, the longitudinal reinforcement ratio was kept constant, equal to 0.7%. No. 6 (19 mm, bottom reinforcement) and No. 4 (12.7 mm, top reinforcement) bars with respective yield strengths of 66 ksi (455 MPa) and 77 ksi (531 MPa). These bars were used as longitudinal reinforcement in the members. However, No. 3 (9.5 mm) bars with a yield

strength of 74 ksi (510 MPa) were used as shear reinforcement (stirrups) to prevent a shear failure mode prior to flexural failure.

The SRP system consisted of twisted high carbon steel cord (Hardwire® Tape Galvanized 3X2-12-12) embedded into adhesive epoxy. The twisted high carbon cord consists of three straight steel wires surrounded by two wires wrapped at a high twist angle. Medium density tapes (12 wire per inch) were selected in this study. These tapes will add additional reinforcement and still offer exceptional wet through [9]. The adhesive epoxy (sikadur® 330) was the curing agent used for bonding the steel wires to the concrete substrate. It consists of two components, A and B, which are mixed at a weight ratio of 4:1 and stirred until a homogenous mixture [10].

The control and repaired beams were instrumented to measure the applied load, mid-span beam deflection, and strain in the SRP system. In the control beam, a linear strain gauge was adhered to the steel reinforcement in the mid-span location. In the repaired beams, the linear strain gauges were adhered to the bottom surface of steel fiber in main SRP laminate at mid-span, right end, and left end. Additional strain gauges were positioned on the bottom face of the middle U-wrap in the repaired beams with U wraps and vertically on the right and left sided U-wraps. Linear variable displacement transducers (LVDTs) were attached to the beam well below the compression zone to measure the midspan deflection. Both strain gauges and LVDTs were connected to a data acquisition system where strains, beam deflection, and load information were recorded.

All the beams were simply supported and tested in a four-point bending configuration, as shown in **Fig. 1**. The load was applied by two 140 kips (620 kN) servo-hydraulic actuators. The actuators were intended to apply the two-point loads to the beams. The load was applied using a displacement rate of 0.050in./min (1.27 mm/min), and the automatic data acquisition system recorded data every second.



**Fig. 1.** Test setup.

Prior repair and strengthening, the beams were tested to failure to simulate the condition of a damaged beam. Damaged area in the beams was repaired first by repairing damaged concrete before applying the SRP laminates to the concrete surface. The beams were placed upside down (i.e. rotated 180 degrees) where the beams' soffit could facilitate the repair work in the laboratory. The deteriorated and cracked concrete around and underneath the reinforcement was removed using a pneumatic hammer until sound concrete was reached. A wire brush was utilized to clean the rebar from any cementitious materials to provide a better bond with the new repairing materials. Higher pressure air jet was used to remove the dust and the loose particles from the surface. The surface area was then moistened prior to the placement of repairing concrete. High early strength concrete with a compressive strength of 6500 psi (45 MPa) at three days was used for repairing the damaged concrete which was removed. Prior to application of the SRP system, the concrete surface was sandblasted.

Concrete surface preparation was completed on the surfaces where the SRP laminates and U-wraps were applied. Sharp corners in locations of U-wrapping strips were rounded by 1.5 in. (38 mm) to reduce concentrated stresses at the edges of the corner locations. The application of the SRP laminate and the U-wraps followed the manufacture's specification. The repairing process of the beams is illustrated in Fig. 2.

## Results and discussion

### General behavior

Table 1 summarizes the ultimate load capacities, maximum recorded strains, beams' deflection at failure, and the failure mode of each beam. A comparison between the failure load of the control beam (undamaged/unrepaired with SRP) and the repaired beams with SRP showed a restoration in the beams' load capacity based on the retrofitting configuration.

Table 1. Specimen properties and test results.

Beam ID and Configuration	Laminate Area, $A_g$ (in <sup>2</sup> )	$P_{ult}$ , kips	Strain at Ultimate load, in./in.	Max Deflecti on at failure, in.	Failure Mode
Beam-1	0L-0U	103	12629	1.93	Flexural (Steel Yielding)
Beam-2	1L-0U	71	2107	0.076	Delamination
Beam-3	1L-3U	81	1609	0.232	Delamination
Beam-4	2L-3U	95	3447	0.31	Delamination
Beam-5	1L-5U	101	4493	0.344	Delamination and SRP Rupture
Beam-6	2L-5U	117	14345	0.515	Delamination

Note: All beams constructed with the average concrete compressive strength of 6370 psi, L represents the main SRP layer and U represents U-wrap.

The retrofitted beam (beam-2) restored around 70% the load capacity of the control beam. The retrofitted beams with longitudinal SRP laminates and U-wraps (beam-3 and beam-4) restored around 79% and 92% of the load capacity of the control beam, respectively. Duplicating the longitudinal laminate area in the retrofitted beam (beam-5) with three distributed U-wraps restored the full load carrying capacity of the control beam. Moreover, the retrofitted beam (beam-6) with five distributed U-wraps carried 113% the load capacity of the control beam. The structural behavior of the control beam was different than that of the repaired beams. The control beam experienced a classic flexural failure initiated by yielding of the internal reinforcement and excessive deflection [1.93 in. (49 mm)] at the end of the test. In contrast, the retrofitted beams experienced a brittle failure mode as the internal reinforcement was spliced at the higher moment region. So, the retrofitted beams had less deflection values at the failure stage. However, increasing the provided SRP laminate in areas with well distributed U-wraps extended the beams' load

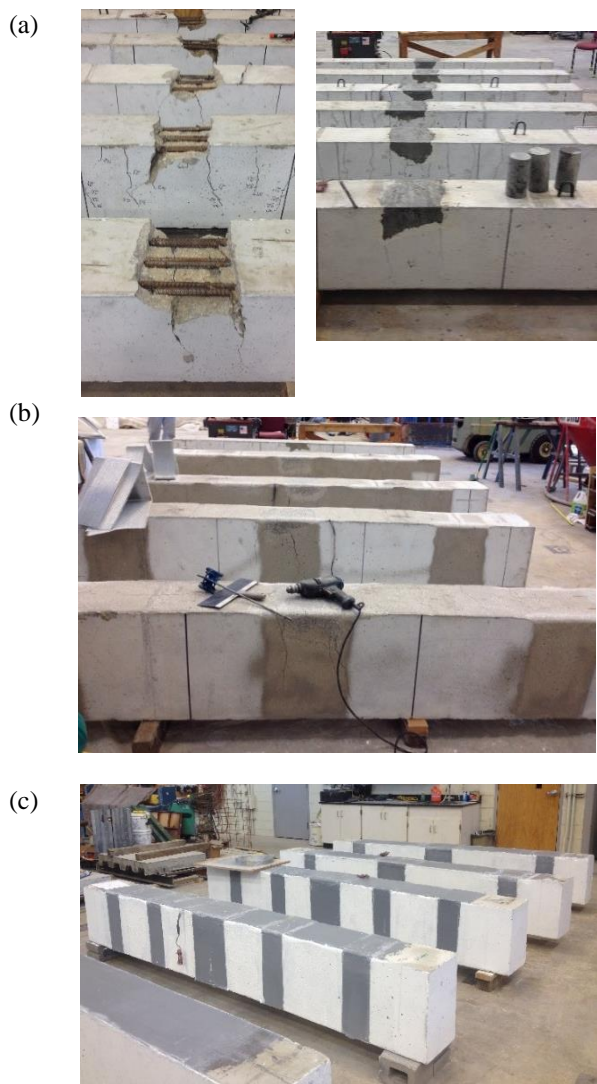


Fig. 2. (a) Repairing the damaged area, (b) Beams prior to external repair system application, (c) Application of the SRP system.

capacity with a significant deflection value. The U-wraps system was very effective in this case study as it provided a confinement to the retrofitted beams. This confinement supported the longitudinal SRP laminates to develop more load capacity before it failed.

### Crack pattern and failure modes

**Fig. 3** represents the tested beams' images after reaching their peak failure. The control beam (beam-1) exhibited typical flexural cracks through testing. The flexural cracks started to propagate at the middle span and increased towards the ends. The cracks became wider as the applied loads increased. The failure mode was observed by yielding of the internal reinforcement followed by concrete crushing, as shown in **Fig. 3-a**.

The repaired beams experienced different modes of failure than the control beam. As the damaged beams were simulated by spliced internal reinforcement at the higher moment regions, no yielding of the internal reinforcement was exhibited. The retrofitted beams had a local failure at the maximum moment region. The failure of the repaired beam (beam-2) demonstrated by delamination of the repaired mortar and the SRP laminate, as shown in **Fig. 3-b**. Then, a debonding of the SRP laminate was exhibited at the peak load and extended toward the beam ends. All other repaired beams that retrofitted with the SRP laminates and the U-wraps had a debonding mode of failure. The debonding of the SRP system started at the midspan of the beams, as shown in **Fig. 3-c, 3-d, 3-e, and 3-f**. Then, the debonding of the longitudinal SRP laminates was extended through the beams' span. However, the two U-wraps located at each beam' ends did not observe any failure and were able to prevent the endplate debonding of the longitudinal SRP laminates. Increasing the U-wraps to five in the repaired beam (beam-5) with one-layer laminate was able to develop almost the full capacity of the SRP system. Therefore, a splitting and separation of the epoxy adhesive system was observed as the steel cords reached its high tensile strength in the U-wraps, as shown in **Fig. 3-e**.

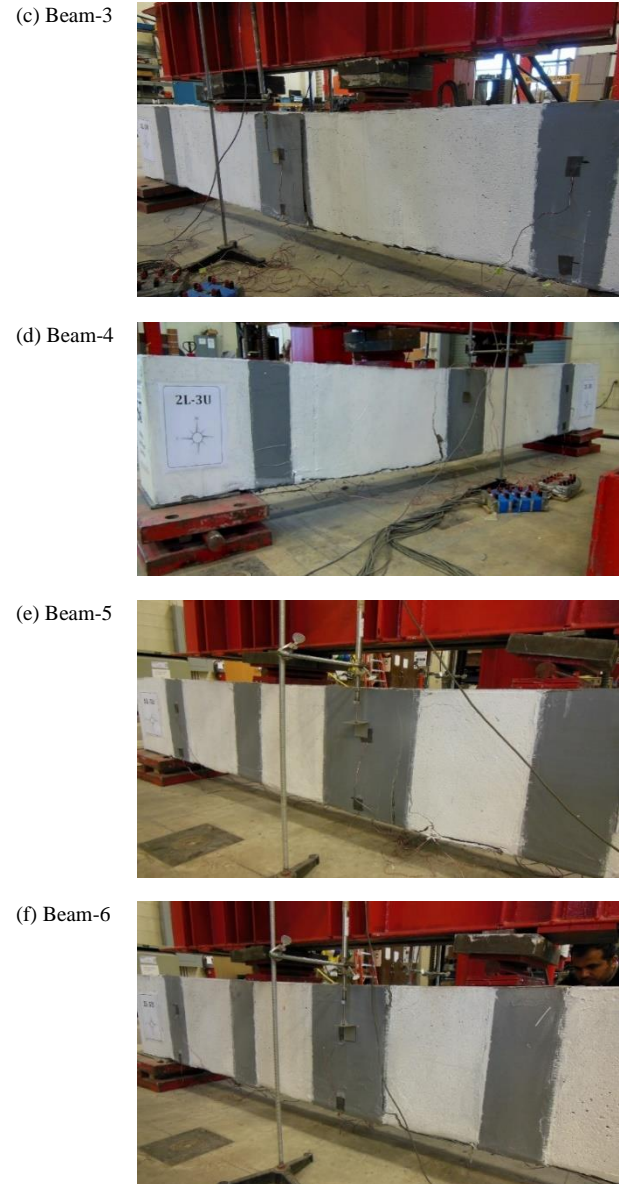


**Fig. 3.** Crack patterns and mode of failures for all tested specimens.

### Load capacity and ductility indices

To examine the efficiency of the SRP repair system, the load capacity and ductility indexes of each beam were determined. The load capacity index is defined as the ultimate load capacity of the repaired beams to that for the undamaged beam (beam-1), as shown in **Table 2**. A comparison between the repaired beams determined that the influence of the SRP system was highly depended on the distribution of the U-wraps. The repaired beam (beam-3) was retrofitted with one layer of SRP laminate and three U-wraps. One U-wrap was installed at the middle span and the other two were at the ends of the beam. The repaired beam (beam-4) was retrofitted as the repaired beam (beam-3) except additional two U-wraps was added through its length. The additional two U-wraps enhanced the load capacity index by 16% in the repaired beam (beam-4) than the load capacity in the repaired beam (beam-3). In addition, increasing the SRP

laminate number to two layers instead of one layer in the repaired beams (beam-4 and beam-5) significantly improved the load capacity by 0.98 and 1.14 of the load capacity in the undamaged beam (beam-1) respectively. The ductility index was also calculated. It is represented as the ratio of the central deflection at the maximum load level of the repaired beams to that of the undamaged beam (beam-1), as shown in **Table 2**. The ductility index of the repaired beam (beam-2) was only 0.04 while the ductility indices of the repaired beams (beam-3 and beam-4) were 0.12 and 0.16, respectively. It is clear that the ductility index was also improved by providing / increasing the number of U-wraps. Moreover, the ductility index was increased to 0.18 and 0.27 by doubling the SRP laminate, as shown in the repaired beams (beam-4 and beam-5), respectively. It should be reminded that the control beam-1 was the only beam with continuous longitudinal reinforcement thus the ductility index values are all rather modest for the discontinuous steel reinforced repaired beams. These test results revealed that the use of the SRP laminates with U-wraps is an effective technique in restoring the load capacity of the severely damaged beams due to over height vehicles collision.

**Table 2.** Load capacity and ductility indices of tested beams.

Beam ID	Load capacity	Ductility
Beam-1	1	1
Beam-2	0.69	0.04
Beam-3	0.79	0.12
Beam-4	0.92	0.16
Beam-5	0.98	0.18
Beam-6	1.14	0.27

**Strain readings**

**Fig. 4** represents the strain readings of the SRP repaired system through the beams’ span at different locations. **Fig. 4-a** represents the strain reading of the SRP main laminates during the applied loads at the beams’ mid-span. In all beams (beam-2, beam-4, beam-5, and beam-6), the load-strain response in the SRP main laminates was similar. In the first stage, the strain was linearly increased as the load applied. The maximum recorded strain in the SRP laminate was observed when the beams reached their maximum peak load. Then, the strain reading continued to increase under the sustained load until the failure occurred. The strain reading was about 0.003 in./in. for the beams that repaired with the SRP laminates plus U-wraps. However, the strain reading was about 0.002 in./in. for the repaired beam without U-wraps.

The strain readings at the left side of SRP main laminates are illustrated in Fig. 4-b. The left side of SRP laminates exhibited less strain reading than that at the mid-span location. The higher recorded strain reading was at the peak loads. After that, no strain readings were recorded at the left side of SRP main laminate in beams (beam-2, beam-4, and beam-5) or the strain readings were continued the same as in beams (beam-3 and beam-

6). The strain readings at the right side were very conceded with the strain reading at the left side of all repaired beams. Also, higher strain readings were announced at the peak load (see **Fig. 4-c**).

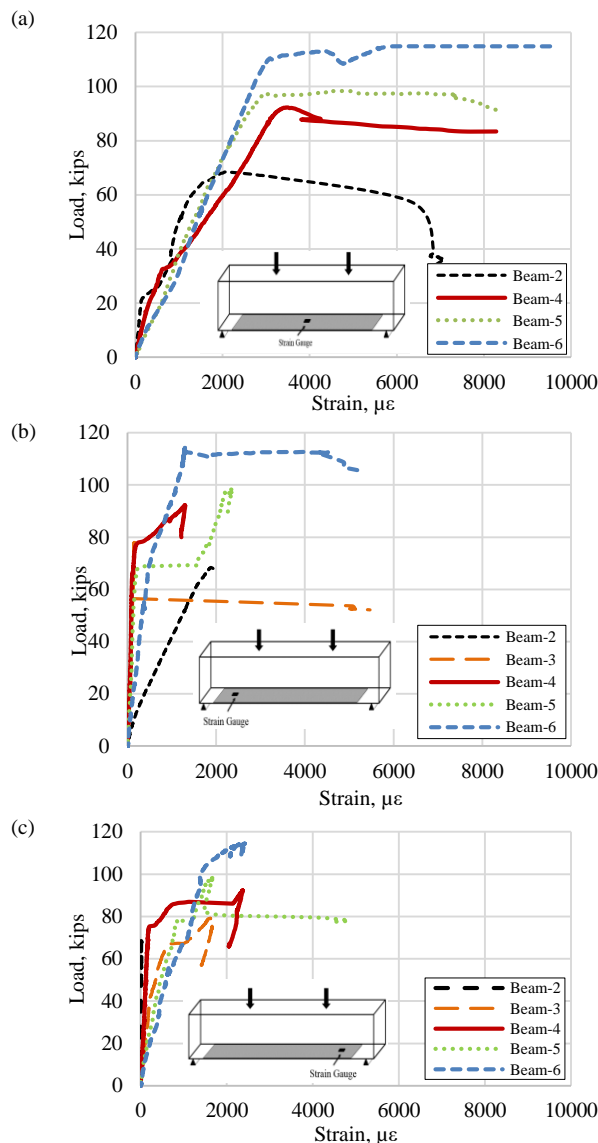


**Fig. 4.** (a) Strain readings at midspan main layer of the repaired beam in addition to the undamaged beam (beam-1), (b) Strain readings at the left side of the main layer, (c) Strain readings at the right side of the main layer.

The strain readings for the U-wraps are shown in **Fig. 5**. For the midspan U-wrap (**Fig 5-a**), no recorded data for the beam-2 was obtained due to data acquisition error. In addition, the strain gauges for repaired beam-3 and beam-5 did not yield accurate strain readings with the applied loads. Strain gauges are sensitive devices and appeared unreliable beyond peak loading perhaps due to test damage. In spite of this, the load-strain response of the U-wraps is well represented for the repaired beam-4 and beam-6. The strain readings for these two beams remained near zero until the applied loads were very close to the peak load. This means that the U-wraps were not active engaged until a sufficient load was applied and the main SRP laminate started to lose its ability in

carrying more loads. Then, the strain readings continued to increase up to the peak load when a sudden drop in the strain readings was observed. The continuity of the strain readings at higher load level represented the confinement action of the U-wraps. The sudden drop in the strain reading represented the delamination or the debonding of the SRP laminate and the U-wraps.

**Figs. 5-b** and **5-c** represent the strain readings at the far ends (left and right) U-wraps. All of the U-wraps at the far ends did not exhibit effective strain readings at the peak loads because the failures of the repaired beams were represented by a local failure at the damaged area (mid-span location).

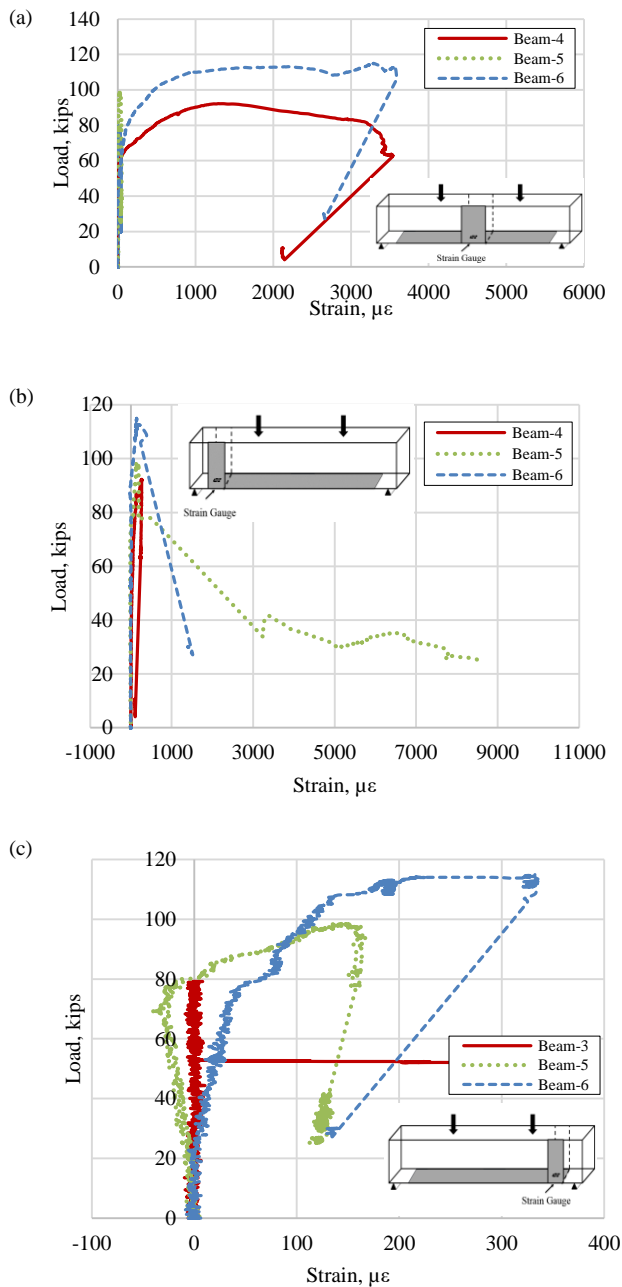


**Fig. 5.** (a) Strain reading at bottom midspan U-wrap, (b) Strain reading at the bottom left far end U-wrap, (c) Strain readings at bottom right far end U-wrap.

## Conclusion

The experimental investigation of repairing damaged RC beams with SRP system showed that the SRP system is a very effective composite material that can be used in restoring/increasing the moment capacity of severely damaged RC beams. Some remarkable points are listed here:

1. The effectiveness of the SRP system was highly depended on the provided U-wraps. The U-wraps had an impact on restoring the load capacity, enhancing the ductility, and providing a saver mode of failure.
2. Increasing the SRP laminates with providing a good distribution of the U-wraps were able to increase in the repaired beam' load capacity by 17% of that in the control beam.
3. The observed failure mode was influenced by the U-wraps. Delamination and debonding through the span length were observed for the repaired beam with the SRP laminate only. While a local debonding in the SRP system (SRP laminate and U-wraps) was exhibited in all other beams that repaired with SRP laminates and U-wraps.
4. The highest strain reading in the SRP main laminate was recorded at the middle span of the repaired beams. The far right and left ends of the SRP main laminate had less strain reading.
5. The middle span U-wraps in the repaired beams had the highest strain reading. While the far right/left side U-wraps exhibited almost zero strain reading at the peak loads. This illustrates the ability of the end U-wraps in preventing the endplate debonding failure mechanism.

## Acknowledgements

The researchers gratefully wish to acknowledge the Department of Civil, Architectural, and Environmental Engineering at Missouri S&T and HCED Iraq sponsor for their support. The authors also want to thank Sika USA Corporation for donating the epoxy agent and Hardwire LLC for providing the steel wire materials used in this study.

## Author's contributions

Conceived the plan: HHA, ZKA, and JJM; Performed the experiments: HHA, ZKA, ZRA; Data analysis: HHA, JJM, and ZRA; Wrote the paper: HHA, JJM, and ZRA. Authors have no competing financial interests.

## References

1. Soudki, K. A., Sherwood, T., & Masoud, S. (2000). FRP repair of corrosion-damaged reinforced concrete beams. Universidad de Waterloo, Canadá.
2. Russo, F. M., Wipf, T. J., Klaiber, F. W., & Paradis, R. Y. A. N. (2000). Evaluation and Repair of Damaged Prestressed Concrete Girder Bridges. In Mid-Continent Transportation Symposium Proceedings (pp. 109-114).
3. Klaiber, F. W., Wipf, T. J., & Kempers, B. J. (2003, August). Repair of damaged prestressed concrete bridges using CFRP. In Proceedings of the 2003 Mid-Continent Transportation Research Symposium, Ames, Iowa.
4. Haddad, R. H., Shannag, M. J., & Moh'd, A. (2008). Repair of heat-damaged RC shallow beams using advanced composites. *Materials and Structures*, 41(2), 287-299.

5. El-Maaddawy, T., & Chekfeh, Y. (2012). Retrofitting of severely shear-damaged concrete t-beams using externally bonded composites and mechanical end anchorage. *Journal of Composites for Construction*, 16(6), 693-704.
6. Zhou, H., & Attard, T. L. (2013). Rehabilitation and strength sustainability of fatigue damaged concrete-encased steel flexural members using a newly developed polymeric carbon-fiber composite. *Composites Part B: Engineering*, 45(1), 1091-1103.
7. Tigeli, M., Moyo, P., & Beushausen, H. (2013). Behaviour of corrosion damaged reinforced concrete beams strengthened using CFRP laminates. In *Nondestructive Testing of Materials and Structures* (pp. 1079-1085). Springer, Dordrecht.
8. Pino, V., Nanni, A., Arboleda, D., Roberts-Wollmann, C., & Cousins, T. (2016). Repair of Damaged Prestressed Concrete Girders with FRP and FRCM Composites. *Journal of Composites for Construction*, 21(3), 04016111.
9. Hardwire LLC, 2017 "3X2 Cord and Tape Specification Sheet," Hardwire LLC, Pocomoke City, MD, USA, [https://secure.hardwirellc.net/\\_urlfiles/docs/hardwire/brochures/hwcord\\_specs/US/3X2G\\_cord\\_US.pdf](https://secure.hardwirellc.net/_urlfiles/docs/hardwire/brochures/hwcord_specs/US/3X2G_cord_US.pdf).
10. Sika USA Corporation (2017) "Sikadur® High-modulus, high-strength, impregnating resin," Sika Corp. Lyndhurst, NJ, <http://www.sikaconstruction.com>.